ISSN 1063-7850, Technical Physics Letters, 2018, Vol. 44, No. 12, pp. 1226–1229. © Pleiades Publishing, Ltd., 2018.
Original Russian Text © G.N. Churilov, N.S. Nikolaev, K.V. Shichalin, V.A. Lopatin, 2019, published in Pis'ma v Zhurnal Tekhnicheskoi Fiziki, 2019, Vol. 45, No. 1, pp. 42–45.

A Plasma Generator with Magnetic Vortex Stabilization and Possibilities of Its Use

G. N. Churilov[a,b,*], N. S. Nikolaev[a,b], K. V. Shichalin[a], and V. A. Lopatin[b]

[a] *Siberian Federal University, Krasnoyarsk, 660041 Russia*

[b] *Kirensky Institute of Physics, Federal Research Center KSC, Siberian Branch, Russian Academy of Sciences, Krasnoyarsk, 660036 Russia*

**e-mail: churilov@iph.krasn.ru*

Received September 21, 2018

Abstract—A design of a plasma generator, the parameters of the resulting plasma, and the possibilities of its use for the synthesis of nanosized powders and optical emission spectroscopy are described. The device operation is based on the arc discharge of alternating current (66 kHz) in an argon jet between water-cooled metal electrodes. The discharge is stabilized by a flow of isolating gas (helium, nitrogen, air) and an axial magnetic field. The gas flow is fed tangentially to the discharge axis. The plasma between the electrodes has the shape of a cylinder remote from the chamber walls. The temperature and electron concentration in the cross section of the plasma cylinder vary along the radius and take the maximum and minimum values.

DOI: 10.1134/S106378501901005X

In recent years, the high-current ac electronics has got impetus in the development (10^4–10^6 Hz). The use of high-frequency (HF) currents made it possible to solve effectively a number of problems: in the field of material synthesis, creation of new sources of electromagnetic radiation and plasma generators, etc. [1–6]. This paper presents the results of investigation of a plasma generator that we developed with a power supply frequency of 66 kHz. It is characterized by low erosion of electrodes and high stability of discharge and the plasma flow formed by it. To obtain a stable plasma flow for the purpose of possible use in the synthesis of nanodispersed powders and optical emission analysis, a plasma generator was developed, manufactured and investigated (Fig. 1). High-frequency discharge *6* occurred between two metal electrodes. Top electrode *1* was fabricated in the form of a ring of copper tube and cooled with water. Bottom electrode *4*, also cooled with water, was made of a copper rod with an axial hole through which argon was fed. The ring has a cut and creates a magnetic field in accordance with the current flowing through it. A similar design was used by us earlier [7].

Part of the discharge plasma stream was exposed to the magnetic field of coil *2*, which caused the stabilization of the discharge and additional heating of the coil. Argon was used as a plasma gas, and nitrogen or helium were used as a stabilizing gas. The plasma-forming argon flow was fed through the axial hole of the central electrode. Stabilizing gas flow *5* was fed tangentially in the plane perpendicular to the plasma gas flow near the end of the central electrode, causing its rotation. Getting into the part of ceramic nozzle *3* of a smaller diameter, the swirling flow of gas is compressed and increases its rotation speed. Next, the plasma flow gets into the magnetic field of the solenoid. The solenoid connected to the primary circuit in series with the arc discharge creates an axial magnetic field in the ceramic part of the chamber with narrow diameter. The reduced pressure resulting from the rotation of the gas stream and the axial magnetic field ensures the localization of the discharge plasma near the axis, as well as the stability of the discharge. Due to this, the Ampere force is constantly acting on the discharge, preventing the current deviation from the axial direction and protecting the wall of the ceramic chamber from overheating and destruction.

The spectral characteristics were measured using a PGS-2 spectrograph with an FEC-9 digital spectra recording system. The discharge temperature was measured by the method of relative intensities of spectral lines using CuI atomic lines of 510.5 and 521.8 nm. Copper powder was injected with a plasma gas (argon) stream, since the lines of copper were not observed without injection. The reason for this phenomenon is discussed further. The electron concentration was calculated using the Stark broadening of hydrogen lines. The chord intensities were recalculated using the Abel transform. Distributions of temperature and electron concentration across the radius of a plasma column were obtained for the whole visible plasma flow (Figs. 2a, 2b). The observed diameter of the plasma jet was

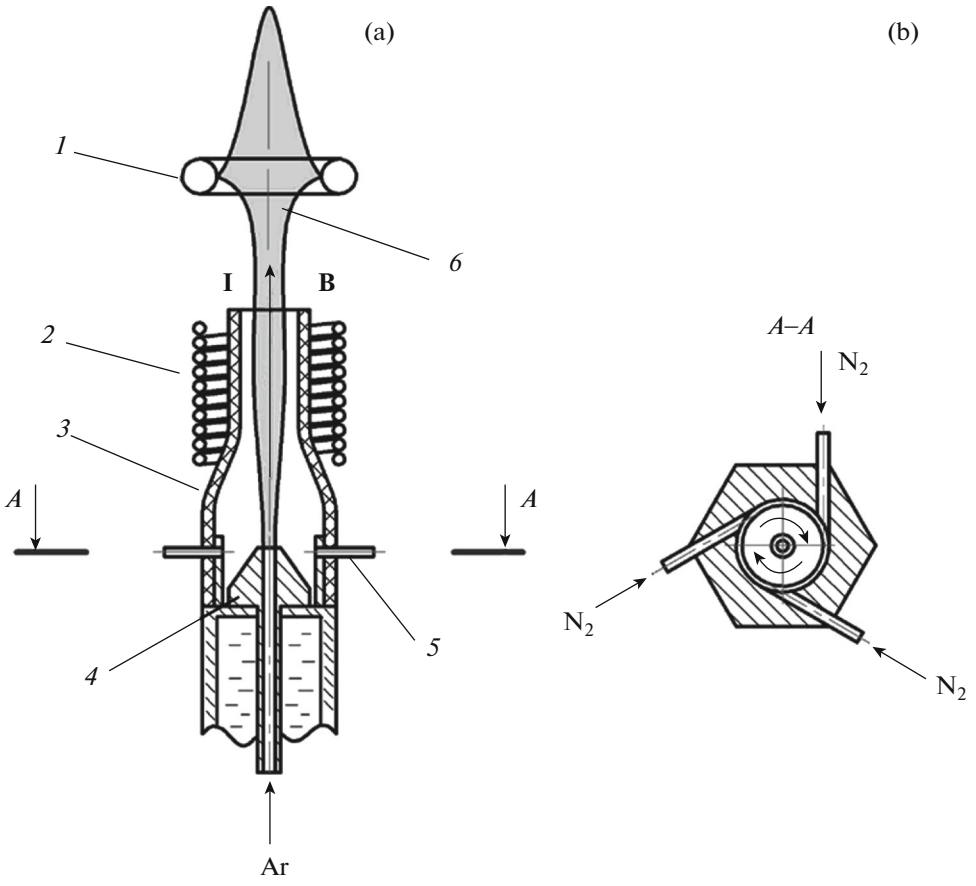

Fig. 1. The design of the plasma generator with magnetic-vortex stabilization of the discharge. (a) Vertical section: vector indicates the directions of current and magnetic induction in the coil (the directions of the discharge current and the magnetic field generated by the solenoid are the same); (b) horizontal section with a stabilizing gas supply scheme.

4.2 mm for a nozzle outlet diameter of 8 mm. As can be seen from the figure, there are coaxial layers with different temperatures and electron concentrations of the plasma flow. Conditionally, we can allocate three areas along the length of the discharge: (I) the central "cold" region at a distance of 0–0.7 mm from the axis, (II) the intermediate cooled" region at a distance of 0.8–1.5 mm, and (III) the extreme "hot" region at a distance of 1.6–2 mm (Fig. 2a). These areas are most clearly visible in the sections located at distances of 2–3.5 mm after start of observation of the discharge. The electron concentration in the same sections varies in a similar way: the maxima are located in the center and at the discharge edge. In this case, at large distances, the axial maximum of the electron concentration is absent, a gradual growth is observed near the edge region of the discharge. For "colder" area *2*, this trend is broken.

Thus, the stabilization of the plasma column arises due to two factors: the radial pressure gradient and the Ampere force of the axial magnetic field. The rotating hot gas creates a region of reduced pressure into which the hottest plasma layers are moving. The axial magnetic field does not allow current to deviate from axial motion along the nozzle channel and touch the nozzle walls due to the Ampere force. The significant difference in the radiation intensities of outer layer III and central layer I indicates the different internal energy of the plasma of these layers. When an arc discharge burns in a plasma flow, plasma is separated into two components with different temperatures and electron concentrations, as well as with different radiation intensities. It was experimentally found that the axial magnetic field and the vortex supply of stabilizing gas separately did not stabilize the plasma flow and inevitably led to the nozzle destruction.

In addition to the results of the study of the spectra of optical radiation given above, the unexpected fact was found that there was no radiation of the material of the electrodes (from copper) in the case in which copper was not specifically introduced (Fig. 3). The signal-to-background ratio is defined as the ratio of the average intensity of radiation determined from three copper lines (510.5, 515.3, and 521.8 nm) relative to the background. As can be seen from Fig. 3a, the maximum signal-to-background ratio (760) is at a distance of 2 mm from the lower end of the electrode if a sample is present in the plasma fed through the axial

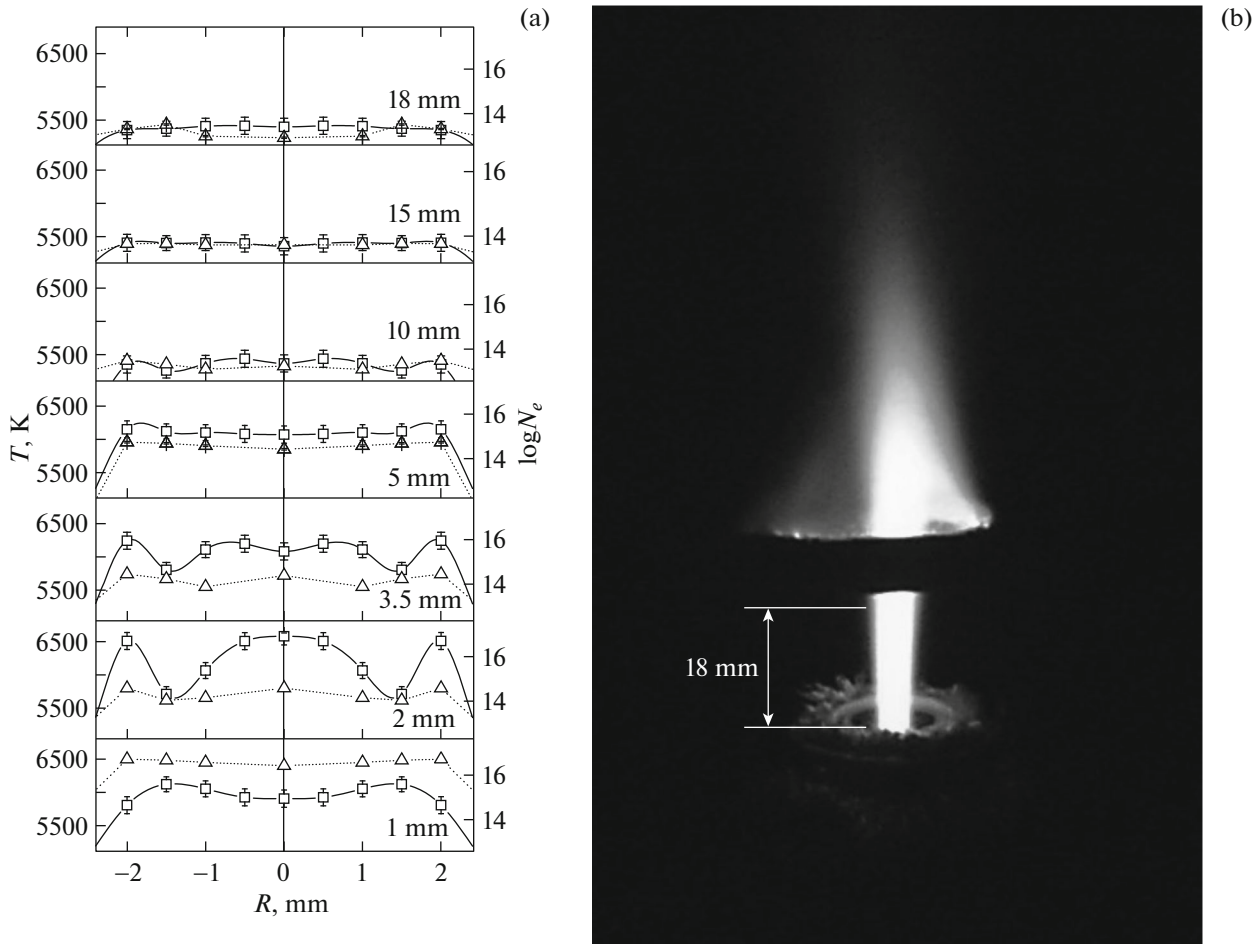

Fig. 2. (a) Temperature distribution (solid line) and electron concentration (dashed line) over the discharge gap; (b) photo of the discharge of the plasmatron with magnetic vortex stabilization; the part of the discharge gap to be measured is marked.

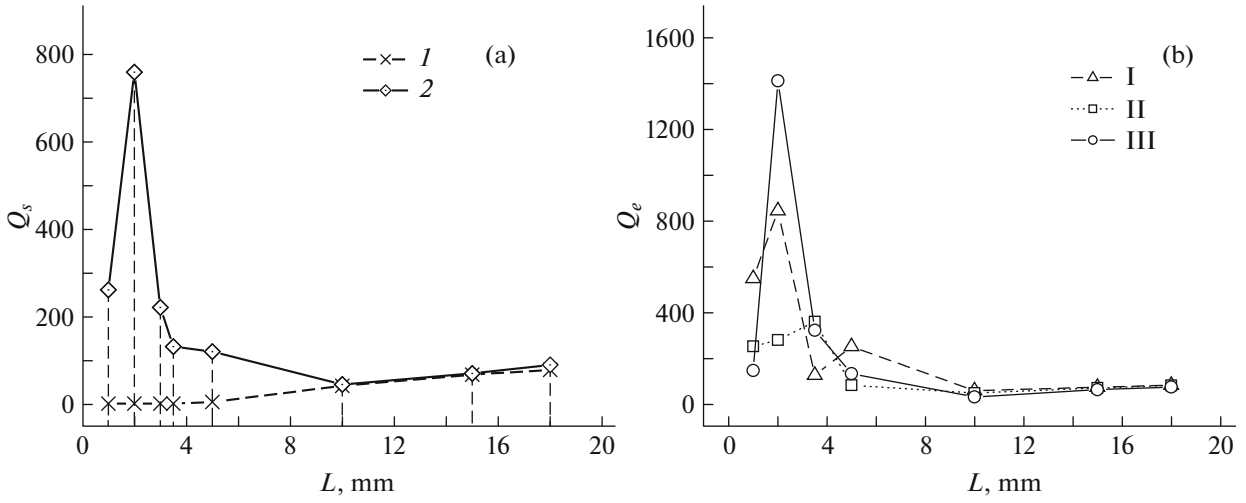

Fig. 3. Distributions of the signal-to-background ratio for the discharge. (a) Q_s is the averaged by chord intensity of the copper lines: (*1*) without Cu, (*2*) with Cu supply to the discharge gap; (b) (Q_e) the average value at the point for different temperature regions (I–III) of the discharge. Relative measurement error is 2.0%.

hole of the electrode. In the case in which there was no sample, the electrode material lines were not observed in the spectrum at altitudes less than 5 mm. Consequently, the electrode material was absent in this region of the plasma jet. When the sample is fed into the discharge gap, the radiation intensity also changes for each of the temperature regions. The maximum signal-to-background ratio (1410) is reached at a distance of 2 mm from the nozzle outlet in edge region *3*.

We earlier established that the erosion of the annular inductor-electrode is only 10^{-12} kg/C and is associated with the action of a strong magnetic field causing a chaotic movement of electrode spots along the electrode surface [8]. However, the end face electrode was always destroyed, although erosion was already 10^{-7}–10^{-8} kg/C. Studies of the powder, which was harvested from the walls of the ceramic chamber during operation of the plasma generator with a stabilizing gas (air), made it possible to establish that the nanodispersed particles are particles of copper oxide. Thus, the central end face electrode is sputtered, collected in particles, and deposited on the inner surface of the cylindrical chamber under the action of centrifugal force.

In conclusion, one can note that the HF arc plasma torch with vortex and magnetic stabilization is characterized by the absence of emission lines of the electrode material and high values of the signal-to-background ratio. Due to this, the device shows promise as a source of light for optical emission spectroscopy. We also showed that it can be used in the synthesis of nanodispersed metallic powders when sputtering the material of the central electrode.

REFERENCES

1. G. N. Churilov, RF Patent No. 2326353 C1 (2008).
2. Yu. V. Blagoveshchenskiy, A. V. Nokhrin, M. S. Boldin, N. V. Sakharov, N. V. Isaeva, S. V. Shotin, O. A. Belkin, A. A. Popov, E. S. Smirnova, and E. A. Lantsev, J. Alloys Compd. **708**, 547 (2017). https://doi.org/10.1016/j.jallcom.2017.03.035
3. P. V. Krasovskii, A. V. Samokhin, A. A. Fadeev, and N. V. Alexeev, Adv. Powder Technol. **27**, 1669 (2016). https://doi.org/10.1016/j.apt.2016.05.031
4. I. V. Karpov, A. V. Ushakov, L. Yu. Fedorov, and A. A. Lepeshev, Tech. Phys. **59**, 559 (2014).
5. I. N. Novikov and A. M. Kruchinin, Tech. Phys. Lett. **40**, 920 (2014).
6. S. P. Zimin, I. I. Amirov, V. V. Naumov, and K. E. Guseva, Tech. Phys. Lett. **44**, 518 (2018).
7. G. N. Churilov, V. A. Lopatin, P. V. Novikov, and N. G. Vnukova, Instrum. Exp. Tech. **44**, 519 (2001).
8. N. G. Vnukova, Cand. Sci. Dissertation (Krasnoyarsk, 2003).

Translated by G. Dedkov